SONIC ANEMOMETER TILT CORRECTION ALGORITHMS

JAMES M. WILCZAK[1], STEVEN P. ONCLEY[2] and STEVEN A. STAGE[3]
[1]*National Oceanic and Atmospheric Administration, Environmental Research Laboratories, Environmental Technology Laboratory, Boulder, CO 80303, U.S.A.;* [2]*National Center for Atmospheric Research, Boulder, CO 80303, U.S.A.;* [3]*Innovative Emergency Management, Baton Rouge, LA 70809, U.S.A.*

(Received in final form 4 July 2000)

Abstract. The sensitivity of sonic anemometer-derived stress estimates to the tilt of the anemometer is investigated. The largest stress errors are shown to occur for unstable stratification ($z/L < 0$) and deep convective boundary layers. Three methods for determining the tilt angles relative to a mean streamline coordinate system and for computing the tilt-corrected stresses are then compared. The most commonly used method, involving a double rotation of the anemometers' axes, is shown to result in significant run-to-run stress errors due to the sampling uncertainty of the mean vertical velocity. An alternative method, requiring a triple rotation of the anemometer axes, is shown to result in even greater run-to-run stress errors due to the combined sampling errors of the mean vertical velocity and the cross-wind stress. For measurements over the sea where the cross-stream stress is important, the double rotation method is shown to overestimate the surface stress, due to the uncorrected lateral tilt component. A third method, using a planar fit technique, is shown to reduce the run-to-run stress errors due to sampling effects, and provides an unbiased estimate of the lateral stress.

Keywords: Anemometers, Coordinate systems, Sloping terrain, Surface layer, Tilt corrections.

1. Introduction

The fact that large errors in the measurement of the horizontal momentum flux can result from relatively small errors in the alignment of turbulent wind sensors has long been known (Pond, 1968; Deacon, 1968; Kaimal and Haugen, 1969; Dyer and Hicks, 1972; Dyer, 1981). The source of the large momentum flux errors is the cross contamination of velocities that occurs in a tilted sensor, such that fluctuations in the longitudinal components of the wind appear as vertical velocity fluctuations, and vice versa.

In level terrain the most straightforward solution is to be certain that the turbulent wind sensors are exceedingly close to being in the true horizontal and vertical planes. Kaimal and Haugen (1969) suggest that in perfectly level terrain the anemometers be leveled to within 0.1 degree. Alternatively, if the magnitude of the tilt of the sensor is known to a similar 0.1 degree accuracy, the measured velocity time series (and average stress) can be corrected in a post analysis to the true horizontal/vertical coordinate system. In either case, a very accurate inclinometer is required, and the terrain must be level to a small fraction of a degree.

Boundary-Layer Meteorology **99:** 127–150, 2001.

In many micro-meteorological field programs, the local terrain is not level to this precision. Over sloping terrain the most useful coordinate system for the analysis of surface-layer turbulence data is a mean streamline coordinate system. For measurements close to the surface in gently sloping terrain, so that flow separation is avoided, the mean streamlines will closely parallel the terrain, and the mean streamline coordinate system can also be considered to be a terrain-following coordinate system. Therefore, in the mean streamline coordinate system the x-axis is parallel to the local mean wind; the z-axis is orthogonal to x, and perpendicular to and up from the plane of the local terrain; and the y-axis lies in the plane of the local terrain in such a direction that a right-handed coordinate system results.

There are several reasons for the choice of a streamline coordinate system in sloping terrain. The first is to make the data readily comparable to analytical theories, which are most easily cast in the streamwise coordinate system (Finnigan, 1983, 1992; Kaimal and Finnigan, 1994).

The second reason is to generate parameterizations that minimize the effect of the sloping terrain, so that results are easily comparable to measurements taken over a flat surface. If an anemometer is placed in a true vertical coordinate system over sloping terrain, fluctuations in the streamwise velocity will create large apparent stresses that are a function of the slope angle relative to the wind direction, and comparison to turbulence measurements over flat terrain would be difficult. If instead the surface-layer turbulence data are analyzed in a coordinate system aligned with the mean streamlines, the variance of the alongslope wind will not produce an apparent stress. The stress in the streamwise coordinate system will then be independent of terrain slope and direction to first order, and can be compared to level terrain results.

One caveat to this approach is that it neglects the effect the terrain slope will have on altering the shape of the low-level wind profile in the presence of diabatic effects, which will modify the surface-layer flux-profile relations. Surface heating or cooling generates horizontal pressure gradient forces (PGFs) that create upslope or downslope flows. In the case of the convective boundary layer, where surface heating typically warms a deep boundary layer, the height scale for the slope-induced PGF will be large, so that within the relatively shallow surface layer the induced PGF will be nearly constant. The surface layer then experiences a different PGF than it would over level terrain, but the PGF is nearly height-independent, and the flux-profile relations for level terrain will still closely apply. In contrast, for stable boundary layers, the surface cooling may be restricted to a boundary-layer depth not much greater than the surface layer, and a PGF that varies rapidly with height in the surface layer is possible. In this case, utilizing a mean streamline coordinate system will significantly reduce the terrain effects, but noticeable differences from measurements in level terrain may still be possible.

A third reason to use streamline coordinates is to produce turbulence parameterizations that are easily implemented in numerical models. We note that in

numerical weather prediction models that use generalized vertical coordinate systems (e.g., sigma, isentropic, or isobaric) the u and v momentum equations and turbulence parameterization schemes are still defined in a true vertical coordinate system (Pielke, 1984), with only the pressure gradient forces modified to account for the effect of the terrain. This might lead one to conclude that turbulence measurements taken over sloping terrain and parameterization schemes developed from these measurements should also use a true vertical coordinate system. However, the turbulence parameterizations in numerical models are generally independent of terrain slope, and specifically assume that the turbulence is horizontally homogeneous. Over sloping terrain the turbulence is not horizontally homogeneous in a true vertical coordinate system. However, if the turbulence parameterizations are developed and implemented in a streamline coordinate system, then the horizontal homogeneity approximation still applies to first order, and parameterizations can be readily developed for use in numerical models. The effect of sub-grid scale undulations in the topography can then be taken into account in these numerical models through separate commonly used form drag (for neutral or unstable stratification) and gravity wave drag parameterizations (for stable stratification), as discussed by Garratt (1992).

Although there are valid reasons for choosing a streamwise coordinate system in sloping terrain, we note that tilting of the turbulence sensors into a streamwise direction to eliminate flow distortion caused by booms or other supporting structures is insufficient (Oost et al., 1994). Wyngaard (1981) finds that for flow past a circular cylinder, tilting the sensors into the streamwise direction only reduces the flow distortion errors by approximately 50%. To properly account for flow distortion, analytic, numerical, or laboratory derived corrections should be applied.

Finally, we note that in some circumstances, the problem of stress measurement applies to cross-stream as well as to the along-stream components. By using K-theory, the lateral stress can be related to the lateral shear of the mean wind. In the baroclinic boundary layer the cross-stream mean wind shear and stress can be significant (Lenschow et al., 1980). However, for surface-layer measurements, it is generally presumed that the lateral shear is small compared to the longitudinal shear, even in strongly baroclinic conditions, and that $|\overline{vw}| \ll |\overline{uw}|$. In contrast, over the sea the cross-stream stress need not be small if the surface wave field propagates in a direction different from the mean wind. Measurements of cross-stream stresses over the sea have been reported (Geernaert, 1988), including measurements of momentum transport from the wave field to the atmosphere when the mean wind field is near calm (Grachev and Fairall, 2001). Therefore, stress measurements over the sea present the additional complication that both the longitudinal and cross-stream stress components are of interest, and the effect of instrument tilt on both components must be considered.

In this paper we review the equations for determining turbulence covariance errors for sensors that are tilted relative to the streamline coordinate system. We then contrast three methods for aligning turbulent wind sensors in the mean streamline

direction, and consider the effect of mean and turbulence sampling errors on the determination of the streamwise coordinate system, and on the streamwise and cross-stream components of the stress. The advantages and disadvantages of each method are discussed for field measurements taken both over land and at sea.

2. Coordinate Transformation Equations

Equations for the conversion of the mean wind and stress components between two orthogonal coordinate systems with different orientations, presented in the context of assessing anemometer tilt angles, were first given by Tanner and Thurtell (1969), and later by Hyson et al. (1977). Here we present the equations for the conversion between two coordinate systems using a matrix formulation, including a discussion of the approximations involved in their derivation.

Equations for the transformation of velocities measured in the coordinate system x, y, z with unit vectors **i**, **j**, **k** to a rotated system x', y', z' with unit vectors **i**′, **j**′, **k** can be expressed (Goldstein, 1981) as

$$\begin{bmatrix} u' \\ v' \\ w' \end{bmatrix} = \mathbf{A} \begin{bmatrix} u \\ v \\ w \end{bmatrix}, \tag{1}$$

where **A** is a 3×3 matrix of the direction cosines between the two coordinate systems, i.e.,

$$A_{11} = \cos(\mathbf{i}', \mathbf{i}) = \mathbf{i}' \cdot \mathbf{i}$$

$$A_{12} = \cos(\mathbf{i}', \mathbf{j}) = \mathbf{i}' \cdot \mathbf{j} \quad \text{etc.}$$

Because the matrix **A** is a rotation, only 3 of the 9 elements of the array are independent. The matrix is most often specified by three Euler angles, α, β and γ, defined as three successive angles of rotation about a choice of three non-parallel axes of rotation. Various conventions exist on the choice and order of these axes of rotation. A convention that is well suited for small angular differences between the two coordinate systems is one in which each rotation is about a different principal axis (Goldstein, 1981). For application to anemometer tilts, we define the first rotation angle α as the pitch angle about the original y-axis; the second rotation is the roll angle β measured about the new or intermediate x-axis; and the yaw angle is the final rotation γ about the new z-axis (Figure 1). In each step a positive rotation angle is defined as being a clockwise rotation when looking down the axis of rotation toward the origin, from the original to the transformed coordinate system. We refer to this rotation order as the "yxz" convention. For each of these

three rotations, the effect of the rotation can be expressed in terms of the rotation matrices **D**, **C**, and **B**, given by

$$\mathbf{B} = \begin{bmatrix} \cos\gamma & -\sin\gamma & 0 \\ \sin\gamma & \cos\gamma & 0 \\ 0 & 0 & 0 \end{bmatrix}, \quad \mathbf{C} = \begin{bmatrix} 1 & 0 & 0 \\ 0 & \cos\beta & -\sin\beta \\ 0 & \sin\beta & \cos\beta \end{bmatrix},$$

$$\mathbf{D} = \begin{bmatrix} \cos\alpha & 0 & \sin\alpha \\ 0 & 1 & 0 \\ -\sin\alpha & 0 & \cos\alpha \end{bmatrix}. \tag{2}$$

The direction cosine matrix **A** given by

$$\mathbf{A} = \mathbf{BCD} \tag{3}$$

represents the combined effect of these three sequential rotations.

We note that to be exact one must measure the pitch and roll angles in the same order as the matrix multiplication in Equation (3), as **A** changes with the order of placement of the **B**, **C** and **D** matrices because matrix multiplication is not commutative. Fortunately, for small rotation angles, different orders of rotations result in small differences in the direction cosine matrices. For example, for tilt angles $\alpha = 1°$, $\beta = 2°$, and $\gamma = 0°$, the difference in measured stresses between the yxz convention and a xyz order of rotation can be shown to be less than 0.1% of the true stress. Thus, for most reasonable situations of tilted anemometers, the order of application of the pitch and roll angles is not important. However, for tilt angles of $\approx 10°$, a change in the order of correction of α and β can produce a change in the 'corrected' stress that is as large as 10% of the true stress.

In contrast to pitch and roll angles α and β, the rotation angle γ will generally be large, as it represents the azimuthal rotation of x and y about z to force $\bar{v} = 0$. The matrix **A** therefore will be sensitive to the position of the rotation matrix **B** relative to **C** and **D**. Consistent with our definition of α and β as being the fixed angles necessary to rotate the sonic into a plane parallel to that of the local terrain slope, the azimuthal rotation must be applied last. If it were applied first, then different α's and β's would be found for each occurrence of a different wind azimuth direction.

For correction of a tilted anemometer, let us associate the primed coordinate system defined in Equation (1) with the measured velocities, u_m, v_m, and w_m, and the angles α, β and γ with the ordered rotations necessary to place the anemometer in a streamwise coordinate system. Since the matrices **B**, **C**, and **D** are orthogonal, so is matrix **A**, and the inverse of **A** is equal to its transpose, $\mathbf{A}^{-1} = \mathbf{A}^T$ so that

$$\begin{bmatrix} u_m \\ v_m \\ w_m \end{bmatrix} = \mathbf{A} \begin{bmatrix} u \\ v \\ w \end{bmatrix} \quad \text{and} \quad \begin{bmatrix} u \\ v \\ w \end{bmatrix} = \mathbf{A}^T \begin{bmatrix} u_m \\ v_m \\ w_m \end{bmatrix}. \tag{4}$$

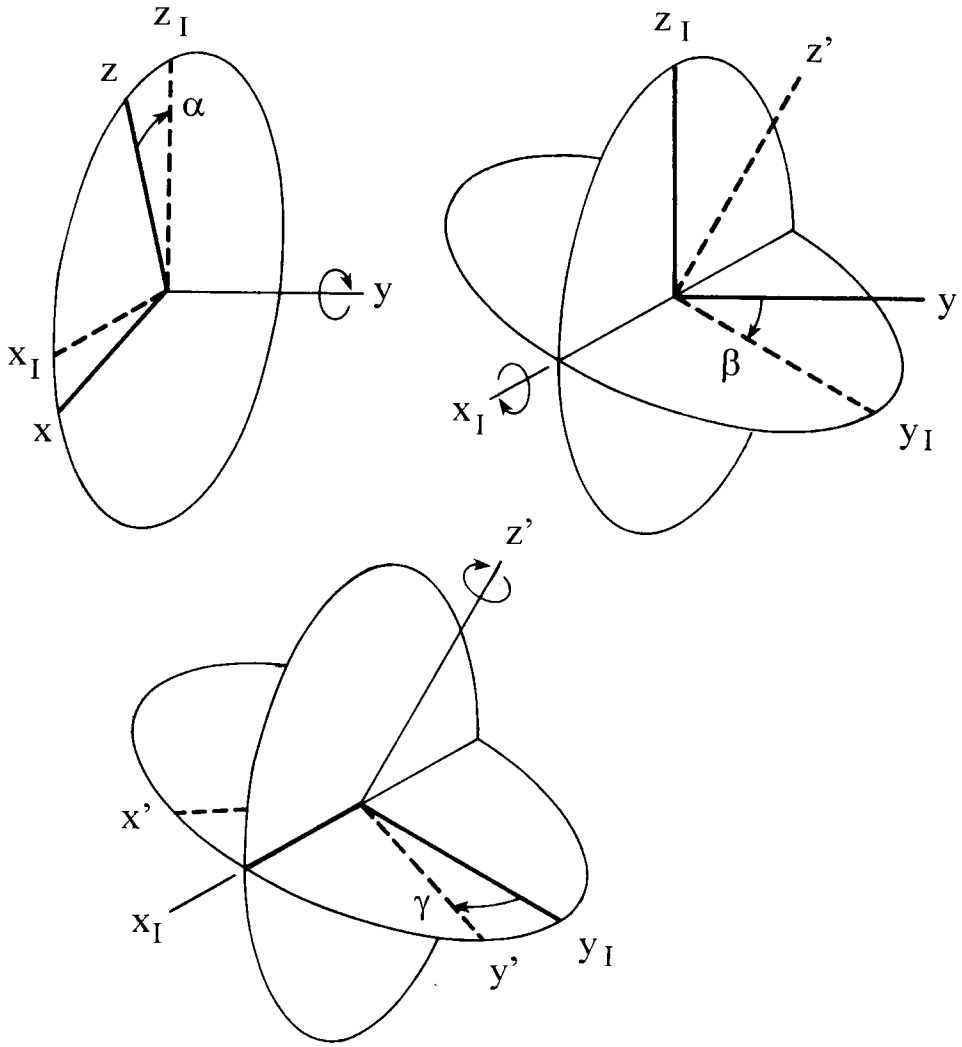

Figure 1. Definitions of the tilt angles α, β, and γ for the yxz convention. The original axes are x, y, z, the final axes are x', y', z', and intermediate axes are x_I, y_I, z_I.

We note that Equation (4) is then equivalent to the set of rotations specified by Hyson et al. (1977).

In place of the ordered pitch and roll angles α and β, in micro-meteorological applications inclination angles often are measured, using bubble levels or other similar devices. The inclination angles are the angles between the anemometer's x-axis and the horizontal plane and between the anemometer's y-axis and the horizontal plane, and have no order associated with them. Knowledge of these angles is equivalent to specifying a_{31} and a_{32} in **A**. A third rotation about the true vertical axis to align the mean wind with the x-axis completely specifies **A**. Thus

the inclination angles allow one to directly determine the elements of **A**, without calculating pitch and roll angles as an intermediate step. The resulting rotation matrix, based on inclination angles, can be used to calculate the stress tensor over a flat surface. However, since the inclination angles are measured relative to the horizontal plane, they can not be used to align with mean streamline coordinates over sloping terrain.

In Section 6 we describe a planar fit method that determines the angles between the local slope of the surface and the axes of the sonic anemometer. When this method is used to specify a_{31} and a_{32} in **A** along with a third angle to align the x-axis with the mean wind, the result is a rotation matrix that can be used to find the stress in coordinates aligned with the mean streamlines over either a flat or a sloping surface.

3. Sensitivity of Turbulence Moments to Tilt Angle

We briefly review the sensitivity of stress measurements to tilt angles, considering first the simplified case of a wind along the x-axis, with a tilt only in the x–z plane so that $\gamma = \beta = 0$. Using Equations (2)–(4) and applying a straightforward Reynolds decomposition one obtains the longitudinal and cross stream stress components,

$$\overline{u_m w_m} = \overline{uw}\cos(2\alpha) + \frac{1}{2}(\overline{w^2} - \overline{u^2})\sin(2\alpha), \tag{5}$$

$$\overline{v_m w_m} = \overline{vw}(\cos\alpha) + \overline{uv}(\sin\alpha). \tag{6}$$

Evaluation of Equations (5) and (6) is straightforward given the following empirical relationships for the velocity standard deviations $\sigma_u = (\overline{u^2})^{1/2}$ in unstable conditions (Panofsky et al., 1977)

$$\frac{\sigma_{u,v}}{u_*} = \left(12 - 0.5\frac{Z_i}{L}\right)^{1/3}, \tag{7}$$

$$\frac{\sigma_w}{u_*} = 1.25\left(1 - 3\frac{z}{L}\right)^{1/3}. \tag{8}$$

The longitudinal stress error due to an anemometer tilt of one degree in the x–z plane is shown in Figure 2 as a function of z/L, and z/Z_i. The magnitude of the fractional stress error, defined as $|(\overline{u_m w_m} - \overline{uw})/\overline{uw}|$, is largest for deep, convective boundary layers. At $z/L = -1$ and $z/Z_i = 1/500$, the fractional error is 64%. Since $\sin(2\alpha) \approx 2\alpha$ for small angles, Figure 2 can readily be used to linearly scale the stress error for other small angles (e.g., for $\alpha = 0.1$ degrees, the fractional error is 6.4% at $z/L = -1$ and $z/Z_i = 1/500$).

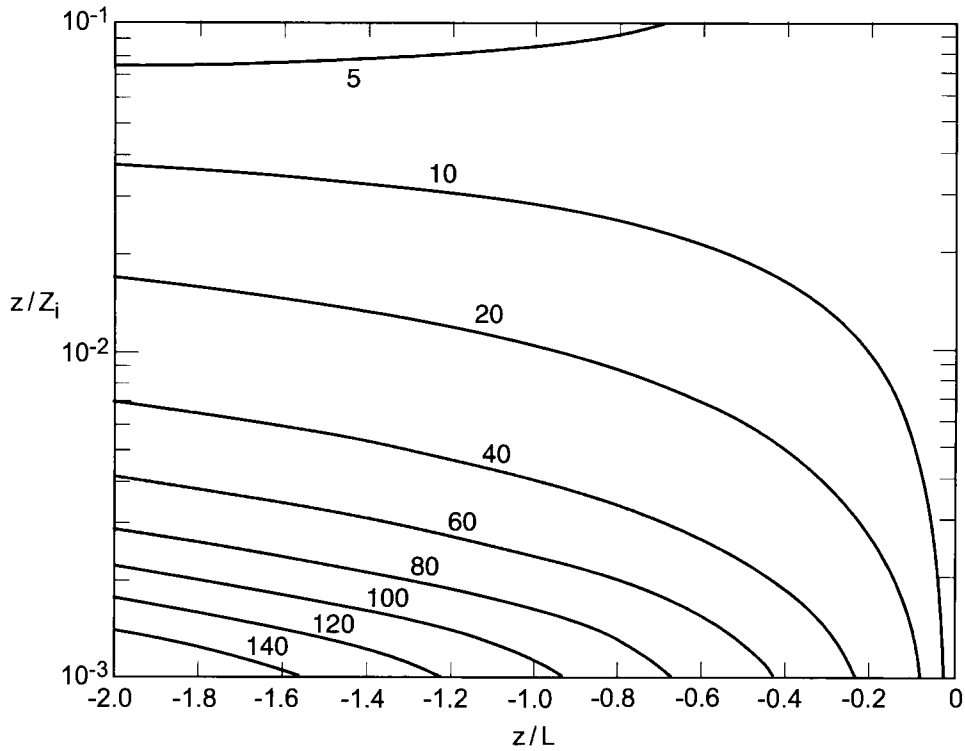

Figure 2. The percent longitudinal stress error as a function of z/L and z/Z_i, for a tilt angle of 1 degree.

The cross-stream stress error expressed as a fraction of the true longitudinal stress, $|(\overline{v_m w_m} - \overline{vw})/\overline{uw}|$, will be dependent on the ratio $\overline{uv}/\overline{uw}$. The ensemble value of this ratio can be non-zero due to spatial variations of surface roughness or to topography. For a single data run averaging period (typically 15 to 60 min), the ratio may also be large due to sampling error, and these sampling errors can result in a significant $\overline{v_m w_m}$. The effects of sampling errors will be discussed further in Section 5.

We note that, if instead the tilt error is assumed to be in the y–z plane only, the longitudinal and cross-stream stress errors become

$$\overline{u_m w_m} = \overline{uw}\cos(\beta) + \overline{uv}\sin(2\alpha), \tag{9}$$

$$\overline{v_m w_m} = \overline{vw}(\cos 2\beta) - \frac{1}{2}(\overline{w^2} - \overline{v^2})\sin(2\beta). \tag{10}$$

In this case the cross-stream stress error is as large as the longitudinal stress error for a tilt in the x–z plane discussed previously. This has important consequences for tilt correction algorithms applied over the sea where the true cross-stream stress may be important, as will be discussed later.

For stable conditions measurements of the velocity variances are inconclusive (Garratt, 1992), and evaluation of Equations (5) and (6) is more difficult. Generally, normalized velocity variances do not differ from their neutral values significantly, in which case errors of approximately 6% per degree of tilt in the x–z and y–z planes are expected for $\overline{uw}$ and $\overline{vw}$.

For completeness we note that assuming $\gamma = 0$ and $\beta = 0$, the relations between the measured and true covariances become

$$\overline{u_m^2} = \overline{u^2}(\cos^2\alpha) + \overline{uw}(2\cos\alpha\sin\alpha) + \overline{w^2}(\sin^2\alpha), \tag{11}$$

$$\overline{v_m^2} = \overline{v^2}, \tag{12}$$

$$\overline{w_m^2} = \overline{u^2}(\sin^2\alpha) + \overline{w^2}(\cos^2\alpha) - \overline{uw}(2\cos\alpha\sin\alpha), \tag{13}$$

$$\overline{w_m T_m} = \overline{wT}(\cos\alpha) - \overline{uT}(\sin\alpha). \tag{14}$$

Normalizing the velocity variances by $\overline{uw}$, the error in the normalized longitudinal and vertical velocity variances is approximately 3.5% per degree. Using the observed heat flux ratio $\overline{uT}/\overline{wT} = -5.4\phi_m\phi_h$ for unstable stratification (Hogstrom, 1990), where $\phi_m = (1 - 19L)^{-1/4}$ and $\phi_h = 0.95(1 - 12z/L)^{-1/2}$ (Hogstrom, 1988), the error in the vertical heat flux goes from approximately 9% per degree of tilt at neutral stability to 1% per degree at $z/L = -1$.

If the tilt error is only in the y–z plane so that $\gamma = 0$ and $\alpha = 0$, the above error equations become

$$\overline{u_m^2} = \overline{u^2}, \tag{15}$$

$$\overline{v_m^2} = \overline{v^2}(\cos^2\beta) - \overline{vw}(2\cos\beta\sin\beta) + \overline{w^2}(\sin^2\beta), \tag{16}$$

$$\overline{w_m^2} = \overline{v^2}(\sin^2\beta) + \overline{w^2}(\cos^2\beta) + \overline{vw}(2\sin\beta\cos\beta), \tag{17}$$

$$\overline{w_m T_m} = \overline{wT}(\cos\beta) + \overline{vT}(\sin\beta) \tag{18}$$

so that over land, where the true value of the ensemble cross-stream stress is expected to be zero, the errors are negligibly small. However, if the measurements are taken over the ocean, errors in the normalized velocity variances will go as approximately 3.5% per degree times the ratio $\overline{vw}/\overline{uw}$.

It is of interest to consider the effects of anemometer tilt on the third order velocity moments that form the turbulent transport term in the TKE budget. Assuming $\gamma = 0$, $\beta = 0$, and neglecting terms $(\sin^2\alpha)$ and $(\sin^3\alpha)$ gives

$$\overline{u_m^2 w_m} = \overline{u^2 w}(\cos^3\alpha) - \overline{u^3}(\sin\alpha\cos^2\alpha) + \overline{uw^2}(2\sin\alpha\cos^2\alpha), \tag{19}$$

$$\overline{v_m^2 w_m} = \overline{v^2 w}(\cos\alpha) - \overline{uv^2}(\sin\alpha) + \overline{uvw}(2\sin\alpha\cos\alpha), \tag{20}$$

$$\overline{w_m^3} = \overline{w^3}(\cos^3\alpha) - \overline{uw^2}(3\sin\alpha\cos^2\alpha). \tag{21}$$

These errors depend on the terms $\overline{u^3}$, $\overline{uw^2}$, $\overline{uv^2}$, and $\overline{uvw}$. The true ensemble values of the last two of these are expected to be small, relative to u_*^2. Wyngaard et al. (1971) have shown that $\overline{uw^2}/u_*^3$ varies from near zero at neutral to approximately -1.5 at $z/L = -1$. Wyngaard and Cote (1971) have shown that $\overline{u^2w}/u_*^3$ and $\overline{w^3}/u_*^3$ vary from near zero at neutral to approximately 2 at $z/L = -1$. Therefore the $\overline{uw^2}$ tilt term will result in a small, approximately 2.5% per degree error in the measurement of both $\overline{u^2w}/u_*^3$ and $\overline{w^3}/u_*^3$. If instead we assume that the tilt error is in the y–z plane, similar values are found for the errors in $\overline{v^2w}/u_*^3$ and $\overline{w^3}/u_*^3$. Although the skewness of longitudinal velocity is small in the surface layer, Chu et al. (1996) find non-trivial values of $\overline{u^3}/u_*^3$, ranging from approximately 0.7 at neutral to -1.7 for unstable stratification. For unstable stratification this will reduce the effect of the already small $\overline{uw^2}/u_*^2$ term in the $\overline{u^2w}/u_*^3$ equation. In summary, for all three components of the TKE turbulent transport term, tilt errors will have a much smaller effect than they do on the stress.

4. Sonic Rotation by Individual Data Run

In the previous section equations were derived allowing for the correction of measured turbulent covariances, given a set of anemometer tilt angles. These angles represent the amount of rotation needed to place the anemometer into the desired coordinate system, which we have taken to be the streamwise coordinate system.

The most commonly applied technique for determining the angles necessary to place the sonic anemometer into a streamwise coordinate system involves a series of two rotations, applied at the end of each turbulent averaging period. This method was first proposed by Tanner and Thurtell (1969), and is described in some detail in Kaimal and Finnigan (1994). The first rotation sets $\bar{v} = 0$ by swinging the x and y-axes about the z-axis so that the new velocities are given by

$$u_1 = u_m\cos\theta + v_m sin\theta, \tag{22}$$

$$v_1 = -u_m\sin\theta + v_m\cos\theta, \tag{23}$$

$$w_1 = w_m, \tag{24}$$

where

$$\theta = \tan^{-1}\left(\frac{\bar{v}_m}{\bar{u}_m}\right) \tag{25}$$

and where subscript 1 denotes the velocities after the first rotation. The second rotation sets $\overline{w} = 0$ by swinging the new x and z-axes about y so that the x-axis points in the mean streamline direction. The final velocities are then given by

$$u_2 = u_1\cos\phi + w_1\sin\phi, \tag{26}$$

$$v_2 = v_1, \tag{27}$$

$$w_2 = -u_1 \sin\phi + w_1 \cos\phi, \tag{28}$$

where

$$\phi = \tan^{-1}\left(\frac{\bar{w}_1}{\bar{u}_1}\right). \tag{29}$$

The above double rotation aligns the x-axis with the mean wind vector, but allows the y and z-axes to freely rotate about x. That is, there are an infinite number of anemometer rotations that simultaneously satisfy $\bar{v} = \bar{w} = 0$. The anemometer's final orientation in the y–z plane after the double rotation depends on its initial orientation. The previous analysis shows that if the error in the y–z plane is only 1 degree then the error in $\overline{vw}$ can be of the same order as the true stress. McMillen (1988) suggests that (over land) a third sonic rotation be applied to remove this ambiguity by requiring that $\overline{vw} = 0$. In this step the new y and z-axes are rotated around x until the cross-stream stress becomes zero, and the third set of rotation equations then become (Kaimal and Finnigan, 1994)

$$u_3 = u_2, \tag{30}$$

$$v_3 = v_2 \cos\psi + w_2 \sin\psi, \tag{31}$$

$$w_3 = -v_2 \sin\psi + w_3 \cos\psi, \tag{32}$$

where

$$\psi = \tan^{-1}\left[\frac{2\overline{v_2 w_2}}{(\overline{v_2^2} - \overline{w_2^2})}\right]. \tag{33}$$

In the context of the rotation matrices discussed in Section 2, the double rotation (DR) method rotates first about the yaw angle, and second about the pitch angle. All of the remaining uncertainty in the tilt is placed into the y–z plane. For the triple rotation (TR) correction scheme, the order of correction is yaw, then pitch, and then roll. We note that the angles ϕ and ψ found by the DR or TR schemes are fundamentally different from α and β defined in Section 2. Whereas α and β are fixed quantities for a given sonic anemometer tilt, ϕ and ψ will depend both on the fixed tilt of the anemometer and on the wind direction.

5. Sampling Error Effects

The double rotation (DR) and triple rotation (TR) tilt correction schemes presented above implicitly assume that the measured mean vertical velocity (and cross-wind stress for TR) are their true ensemble values. However, due to the finite length of the time series for each data run, sampling errors will exist for all turbulence variables. The mean vertical velocity sampling error can be estimated as

$$\bar{w}_{se} = \sigma_w/\sqrt{n}, \tag{34}$$

where n is the number of independent samples of w. The number of independent samples in a time series of length T is given by $n = T/I_s$, where I_s is the Eulerian turbulence integral time scale. For neutral stability I_s scales as $I_s \approx z/\bar{u}$ (Wyngaard, 1973). Thus for z = 10 m, $\bar{u}$ =5 m s^{-1}, T = 15 min, $\sigma_w/u_* = 1.25$, and u_* = 0.3 m s^{-1}, $\bar{w}_{se}$ is 0.01–0.02 m s^{-1}. For unstable stratification the integral scale will be larger. Panofsky and Dutton (1984) suggest that $I_s = 1/(5f_{\max})$, where $f_{\max}$ is the peak of the spectrum plotted as $fS(f)$. Using values of $f_{\max}$ from Kaimal et al. (1972), we find that I_s for unstable stratification can be a factor of 5 larger than at neutral stability. Using $\sigma_w/u_* \approx 2$ for unstable stratification (Wyngaard et al., 1971), we find that $\bar{w}_{se}$ is close to 0.06 m s^{-1}. These numbers agree well with common experience for surface layer data sets.

For a given mean vertical velocity sampling error, both the DR and TR methods will wrongly produce a tilt error correction in the x-z plane given by α_{se} = $\sin^{-1}(\overline{w}_{se}/\bar{u})$. Typical values of $\bar{w}_{se}$ for a 15-min data run can therefore easily produce artificial tilt "corrections" on the order of 0.5 degree. Tilt errors of this magnitude were shown in Section 2 to result in longitudinal stress errors of 10–40% of the true stress for convective boundary layers. The magnitude of this error will tend to be larger for weaker wind speeds because of the dependency of α_{se} on $\bar{u}$.

Sampling errors in $\overline{vw}$ can also lead to erratic corrections for the TR scheme. McMillen (1988) suggests throwing a data run out if the derived correction angle is greater than 10 degrees. Kaimal and Finnigan (1994) suggest applying some sort of smoothing filter to the TR scheme over multiple runs to reduce this effect. However, since the angles ϕ and ψ depend on the wind azimuth, applying such a filter may be problematic when the mean wind direction is changing with time.

So far we have considered the effect of the individual run vertical velocity sampling error on the individual run stress error. The effect of a symmetric distribution of $\bar{w}_{se}$s on a global stress estimate for a series of data runs is next investigated by considering two runs with equal but opposite values of $\bar{w}_{se}$s, with all other mean and turbulent data remaining the same, so that two equal but opposite values of α_{se}s result. From the tilt correction Equation (5), the average stress from these two runs is not the true stress, but the true stress reduced by a factor of $\cos(2\alpha_{se})$. The magnitude of this residual error is for all practical purposes quite small, and the

effect of individual run sampling errors is to produce individual run stress errors without changing the global stress estimate. However, in the extreme situation of light winds and very short averaging times, vertical velocity sampling errors could produce a low bias to the global stress.

6. Planar Fit (PF) Method

A third, relatively unknown, technique for determining the orientation of a sonic anemometer relative to a streamline coordinate system was developed by Steve Stage (1977, unpublished research). Consider a sonic anemometer that is oriented with its vertical axis perpendicular to the local terrain slope, so that its x and y-axes measure the two components of the streamwise flow. If the anemometer is then tilted, we can write

$$\overrightarrow{u}_p = \mathbf{P}(\overrightarrow{u}_m - \overrightarrow{c}), \tag{35}$$

where $\overrightarrow{u}_m$ is the measured wind vector, $\overrightarrow{u}_p$ is the wind vector in a mean streamline coordinate system (not yet rotated into the mean wind direction), **P** is a partial rotation matrix that places the z-axis perpendicular to the plane of the mean streamlines, and $\overrightarrow{c}$ is the mean offset error in the measured winds due to instrument error. The matrix **P** is defined as

$$\mathbf{P} = \mathbf{D}^{\mathbf{T}}\mathbf{C}^{\mathbf{T}}, \tag{36}$$

where matrices **C** and **D** are given by Equation (2). The mean wind components can then be written as

$$\begin{aligned}
\bar{u}_p &= p_{11}(\bar{u}_m - c_1) + p_{12}(\bar{v}_m - c_2) + p_{13}(\bar{w}_m - c_3),\\
\bar{v}_p &= p_{21}(\bar{u}_m - c_1) + p_{22}(\bar{v}_m - c_2) + p_{23}(\bar{w}_m - c_3),\\
\bar{w}_p &= p_{31}(\bar{u}_m - c_1) + p_{32}(\bar{v}_m - c_2) + p_{33}(\bar{w}_m - c_3).
\end{aligned} \tag{37}$$

The mean offset error $\overrightarrow{c}$ is due to the fact that it is extremely difficult to 'zero' the transducers on a sonic to eliminate mean wind speed biases. In practice, the mean bias is often measured by placing an enclosure over the sonic to block the wind. Using this technique it is difficult to achieve an accuracy better than several tens of cm s^{-1}. Although biases on the order of several tens of mm s^{-1} will normally be present in all three velocity components, the tilt coefficients are most sensitive to the vertical component. For example, consider the case of a tilt in the x–z direction of 1.0° with a mean wind of $\bar{u}_m$ = 5 m s^{-1}, which would generate a measured mean vertical velocity of $\bar{w}_m = \bar{u}_m \tan(1°)$ = 0.0872 m s^{-1}. If we now

assume that there exists a $\bar{w}$ bias of 0.02 m s^{-1} and no $\bar{u}$ bias, then the modified tilt angle given by

$$\theta = \tan^{-1}\left(\frac{\bar{w}_m - \bar{w}_{\text{bias}}}{\bar{u}_m - \bar{u}_{\text{bias}}}\right) \tag{38}$$

becomes 0.770° instead of 1.0°. If, however, there are 0.02 m s^{-1} biases in both w and u, then the tilt angle becomes 0.773°. For a range of $\bar{u}$ and $\bar{v}$ of at least 5 m s^{-1} in the data set, the effect of the $\bar{u}$ and $\bar{v}$ mean biases will be negligible, but the $\bar{w}$ bias can be significant. Therefore, the PF method that we recommend contains a mean offset in the measured vertical velocity. The mean offsets in the horizontal components can not be obtained by the PF method, but they do not cause significant contamination in the determination of the rotation matrix.

The mean streamline coordinate system is defined to be aligned so that $\bar{w}_p = 0$. From Equation (37) we then have

$$\begin{aligned} \bar{w}_m &= c_3 - \frac{p_{31}}{p_{33}}\bar{u}_m - \frac{p_{32}}{P_{33}}\bar{v}_m \\ &= b_0 + b_1\bar{u}_m + b_2\bar{v}_m. \end{aligned} \tag{39}$$

The PF method uses wind data and the technique of multiple linear regression to obtain values for b_0, b_1, and b_2. Once b_1 and b_2 are known, there are two possible ways to proceed. The first uses the following relations valid for small inclination angles

$$\begin{aligned} &\tan\alpha = -b_1, \\ &\tan\beta = b_2 \end{aligned} \tag{40}$$

to get

$$\begin{aligned} &\sin\alpha = -b_1/\sqrt{1+b_1^2}, \\ &\cos\alpha = 1/\sqrt{1+b_1^2}, \\ &\sin\beta = b_2/\sqrt{1+b_2}, \\ &\cos\beta = 1/\sqrt{1+b_2^2}. \end{aligned} \tag{41}$$

Substitution of Equation (41) into Equation (36) then gives all of the elements of matrix **P**.

The second approach, valid also for large inclination angles, is to use Equation (39) and the orthogonality condition $p_{31}^2 + p_{32}^2 + p_{33}^2 = 1$ to directly solve for p_{31}, p_{32}, and p_{33},

$$p_{31} = \frac{-b_1}{\sqrt{b_1^2 + b_2^2 + 1}},$$

$$p_{32} = \frac{-b_2}{\sqrt{b_1^2 + b_2^2 + 1}}, \tag{42}$$

$$p_{33} = \frac{1}{\sqrt{b_1^2 + b_2^2 + 1}}.$$

The other components of **P** can then be found by noting that from Equation (36)

$$p_{31} = \sin\alpha,$$

$$p_{32} = -\cos\alpha \sin\beta, \tag{43}$$

$$p_{33} = \cos\alpha \cos\beta,$$

so that

$$\tan\beta = -p_{32}/p_{33},$$

$$\sin\beta = -p_{32}/\sqrt{p_{32}^2 + p_{33}^2},$$

$$\cos\beta = p_{33}/\sqrt{p_{32}^2 + p_{33}^2}, \tag{44}$$

$$\sin\alpha = p_{31},$$

$$\cos\alpha = \sqrt{p_{32}^2 + p_{33}^2}.$$

Substitution of Equations (44) and (42) into Equation (36) gives all of the elements of matrix **P** in terms of b_1 and b_2.

Once the matrix **P** has been found, multiplying the horizontal velocities and stress tensor by **P** places them in the plane of the mean streamlines. These can then be rotated into the mean wind direction for each run through multiplication by the matrix

$$\mathbf{M} = \begin{bmatrix} \cos\gamma & \sin\gamma & 0 \\ -\sin\gamma & \cos\gamma & 0 \\ 0 & 0 & 1 \end{bmatrix}, \tag{45}$$

where

$$\gamma = \tan^{-1}\left(\frac{\bar{v}_p}{\bar{u}_p}\right). \tag{46}$$

The matrix **P** is dependent on the b coefficients, which can be found with the PF method from Equation (39) using multiple linear regression. To find the best-fit plane to the velocity data (the b coefficients), we wish to minimize the function S, where

$$S = \sum_n (\bar{w}_i - b_0 - b_1\bar{u}_i - b_2\bar{v}_i)^2 \tag{47}$$

and where $\bar{u}_i$, $\bar{v}_i$, and $\bar{w}_i$ are the mean velocities for each data run, measured in the sonic anemometer's coordinate system. Differentiating S with respect to b_0, b_1, and b_2 and setting each partial derivative equal to zero results in the three normal equations,

$$\begin{aligned}
nb_0 &+ \left(\sum \bar{u}_i\right) b_1 &&+ \left(\sum \bar{v}_i\right) b_2 &&= \sum \bar{w}_i, \\
\left(\sum \bar{u}_i\right) b_0 &+ \left(\sum \bar{u}_i^2\right) b_1 &&+ \left(\sum \bar{u}_i\bar{v}_i\right) b_2 &&= \sum \bar{u}_i\bar{w}_i, \\
\left(\sum \bar{v}_i\right) b_0 &+ \left(\sum \bar{u}_i\bar{v}_i\right) b_1 &&+ \left(\sum \bar{v}_i^2\right) b_2 &&= \sum \bar{v}_i\bar{w}_i.
\end{aligned} \tag{48}$$

The solution of these three equations provides the linear regression of $\bar{w}_m$ on $\bar{u}_m$ and $\bar{v}_m$. In Appendix A we provide a sample program to solve for the coefficients using matrix notation.

Note that the PF method can only be applied to sets of data when the position of the anemometer does not change. If the anemometer is moved or remounted, or if the bias in the vertical component is adjusted during an experiment, then a separate PF fit must be done for each period between changes. In practice, one can check for changes in the orientation of the anemometer by applying the technique to sub-samples of the entire data set and verifying that the calculated tilt angles do not differ significantly.

In summary, the PF method is applied using the following steps. Compute the mean wind vector and the stress tensor for each run, that is, for each averaging interval, in the sonic anemometer's coordinate system. Perform a linear regression analysis using the components of the mean wind vectors to obtain the coefficients b_0, b_1, and b_2 and then the matrix **P**. Use **P** to obtain the mean wind vectors and stress tensors (or velocity time series) in a coordinate system having its z-axis perpendicular to the mean streamlines. Rotate these intermediate winds and the stress tensor for each run so that the x-axis is along the mean wind and $\bar{v} = 0$. We note that although the vertical velocity averaged over the entire data set is zero, the mean vertical velocities may be non-zero for individual data runs, in large part due

to mesoscale motions or due to sampling limitations. This residual mean vertical velocity is subtracted for each run so that it does not contribute to the Reynolds stress.

7. Applications to the RASEX Data Set

To illustrate differences among the PF, DR, and TR rotation algorithms, we compare stresses calculated using each of the three methods for a single turbulence data set. The data set we use consists of 362 15-min data runs taken during the autumn field campaign of the Riso Air Sea Experiment (RASEX) (Wilczak et al., 1999). The data were taken using an asymmetric Gill Solent sonic anemometer at a height of 10 m, on a sea mast located ≈2 km offshore in water ≈4 m deep. The transducers on the Gill anemometer have an 'hourglass' orientation, but after realtime data processing the anemometer outputs three orthogonal velocities u, v, and w in the sonic relative coordinate system. The data were collected over a range of wind directions from 249° to 325°, that had an open fetch of greater than 15 km. Stresses were computed for each 15-min data run, and then every two consecutive runs were averaged to generate 181 independent stress measurements.

Figure 3a shows the measured mean vertical velocity as a function of the measured $\bar{u}$ and $\bar{v}$ velocity components. It is apparent that the measured $\bar{w}$ velocity increases both with decreasing $\bar{u}$ and increasing $\bar{v}$. Fitting a plane through the data using the routine given in the Appendix results in b_0 = 0.0054 m s^{-1}, $b_1 = -0.0304$, and $b_2 = 0.0188$, so that the tilt angle in the x–z plane is -1.74 degrees, and the tilt angle in the y–z plane is 1.07 degrees. The best-fit plane is found to account for 77% of the variance of the mean vertical velocities. Residual vertical velocities that remain after subtracting the best-fit plane are shown in Figure 3b. The magnitudes of the residual vertical velocities are clearly much smaller, and their distribution is nearly random.

Next we compute longitudinal and lateral stresses for each of the data runs using the three methods. Figure 4a shows the fractional difference in the longitudinal stresses between the PF and DR methods. The mean stresses averaged over the 181 runs are similar (a 3.3% difference), but there is a significant run-to-run variation. This variation increases at smaller values of the stress, which is consistent with the expected run-to-run errors in the DR scheme due to sampling errors of the mean vertical velocity. To determine the origin of the 3.3% mean bias, for each 15-min run we calculate $\alpha_{se} = \alpha_{\mathrm{DR}} - \alpha_{\mathrm{PF}}$, where α_{DR} is the DR method longitudinal tilt angle, and α_{PF} is the PF tilt in the direction of the run mean wind azimuth (Figure 5a). The sign of the 3.3% bias is consistent with that expected for a symmetric distribution of α_{se}s, as discussed in Section 5. However, the average of $|\alpha_{se}|$ is only 0.35 degrees, which is too small to explain the bias. We conclude, therefore, that the bias is due to the limited number of samples (181) in our data set, and that with a much larger data set the bias would decrease to a negligible value.

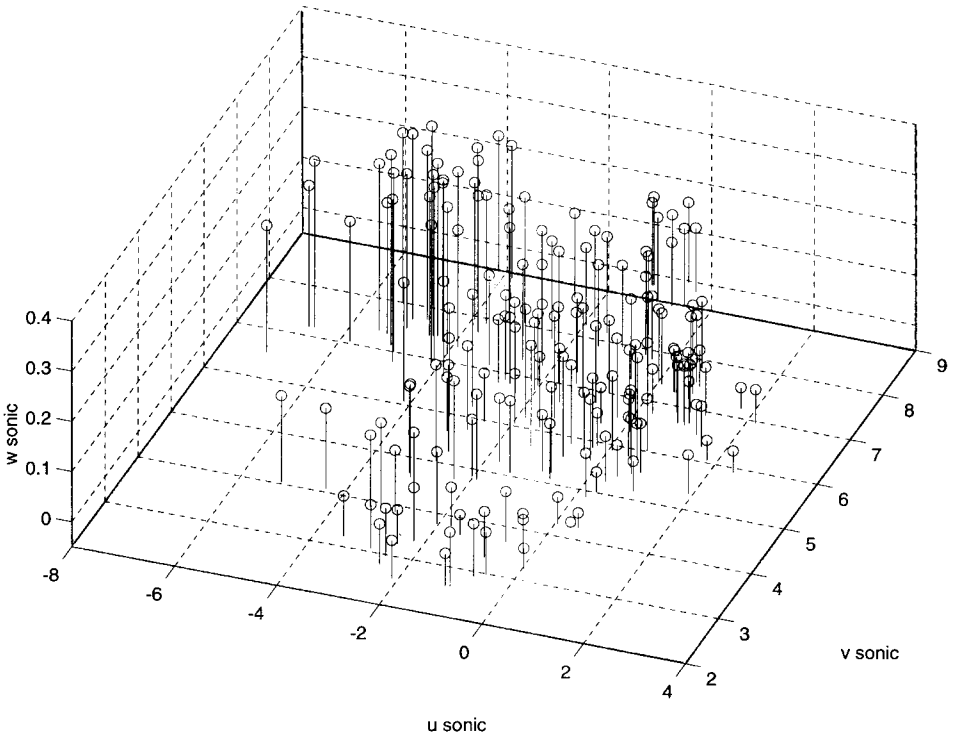

Figure 3a. Mean vertical velocities as a function of horizontal velocities in the sonic anemometer coordinate system (a) as measured, and (b) after subtracting the best fit plane.

In contrast to the longitudinal stress, the cross-stream DR stress (Figure 4b) has a large bias relative to the PF cross-stream stress, averaging 26% of the mean longitudinal stress. This is due to the 1.07 degree y–z tilt component, which is not accounted for in the DR method. This bias can be either sign, depending on the orientation of the anemometer in the y–z plane. Next, the magnitudes of the vector stresses, $(\overline{uw}^2 + \overline{vw}^2)^{1/2}$, calculated with the PF and DR methods are compared in Figure 4d. Because of the bias in the DR cross-stream component, the vector stress bias in Figure 4d has changed relative to the longitudinal stress bias in Figure 4a by 6.7% (from $+3.3$ to -3.4%). The DR method will always provide a larger mean vector stress magnitude than the PF method, because it includes the mean $\overline{vw}$ bias shown in Figure 4b.

Finally, we compare the longitudinal stresses using the PF and TR methods (Figure 4c). With standard deviations of 0.28 and 0.17, respectively (Figure 4a), the scatter of the stress differences has increased compared to those for the PF and DR method. The origin of this greater scatter can be found by examining ψ_{se} for each of the 15-min averages, where $\psi_{se} = \psi_{\mathrm{DR}} - \psi_{\mathrm{PF}}$ (Figure 5b). As before, ψ_{DR} is the value of the lateral tilt computed using the DR method, and ψ_{PF} is the component of the PF tilt perpendicular to the run mean wind azimuth. Typical values of ψ_{se}

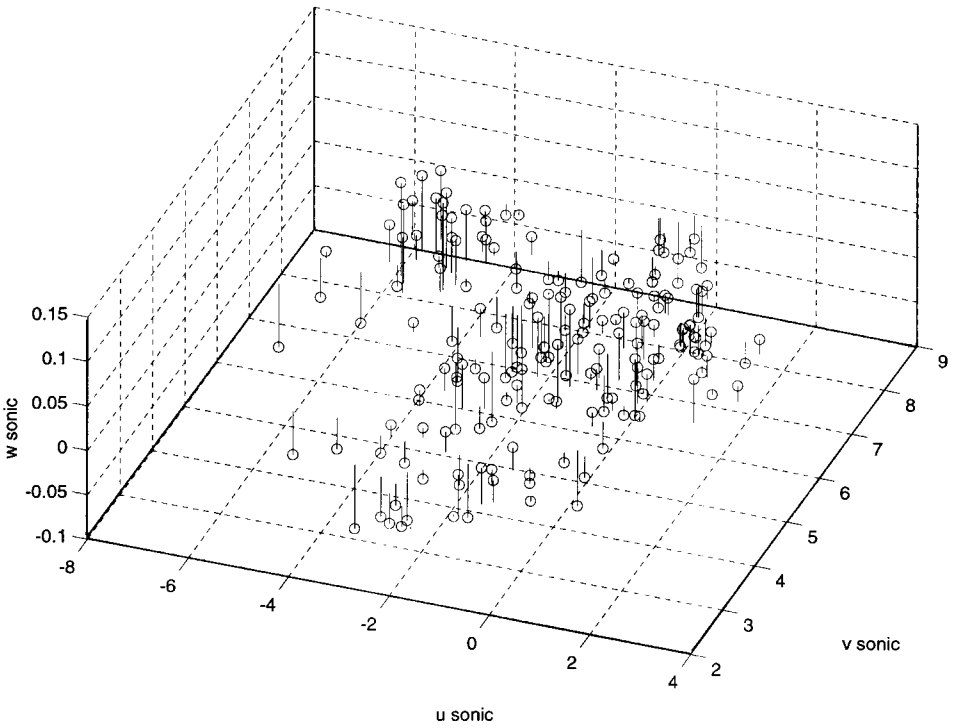

Figure 3b.

are 3–4 degrees, with values frequently exceeding 5 degrees, compared to a typical 1 degree PF lateral tilt. These large, unrealistic tilt angles then change the direction of the z axis in the TR method, and produce greater scatter in the longitudinal stresses.

8. Summary and Discussion

Three different methods for computing the stress from a sonic anemometer have been described and their results compared. The most commonly used method, the double rotation (DR) scheme, is shown to have two disadvantages. The first is that the sampling error of the mean vertical velocity results in a tilt angle estimation error. This adds a random noise component to the longitudinal stress estimate, making individual data run estimates of the stress more uncertain. Second, since the DR method does not correct for the lateral tilt component, large mean biases in the cross-stream stress result, which can be important in applications over the sea. Because of large sampling errors in the measured lateral stress, the triple rotation (TR) method increases the run-to-run noise in the longitudinal stress component.

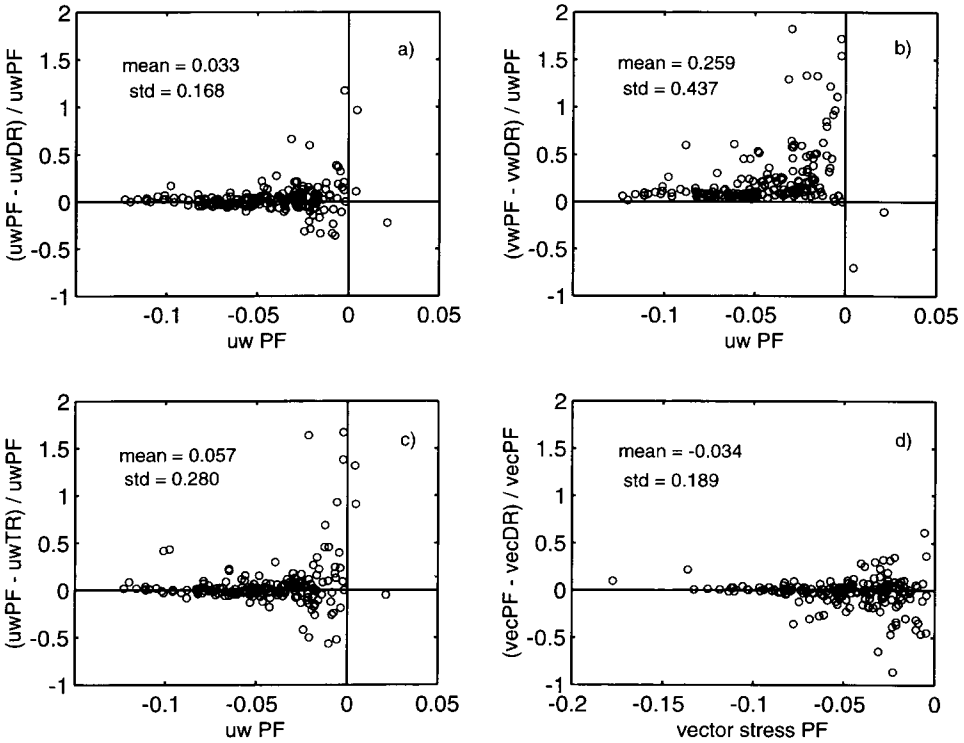

Figure 4. Comparison of stresses using three different methods: (a) differences between the PF and DR longitudinal stresses, normalized by the PF longitudinal stress, as a function of the PF longitudinal stress; (b) differences between the PF and DR lateral stresses, normalized by the PF longitudinal stress, as a function of the PF longitudinal stress; (c) differences between the PF and TR longitudinal stresses, normalized by the PF longitudinal stress, as a function of the PF longitudinal stress; (d) differences between the magnitude of the vector stress between the PF and DR methods, normalized by the magnitude of the PF vector stress.

Also, since it assumes that the true lateral stress is zero, it cannot be used for measurements over the sea where the lateral stress term may be important.

The planar fit (PF) method computes a single set of anemometer tilt angles for a set of data runs. Since many data runs are used to determine the PF tilt angles, it is much less susceptible to sampling errors. The method also allows one to accurately compute the lateral component of the stress. The one disadvantage of the PF method is that it requires that many data runs be recorded before the stresses can be computed. In contrast, the DR and TR methods can be applied in real time to each data run as it is recorded.

Over sloping terrain, the PF method requires that care must be taken that the tilt of the anemometer *and* its orientation relative to the terrain slope do not change over the period of time in which the set of mean velocities has been measured. Over a flat surface, such as the sea, the only requirement is that the tilt of the anemometer does not change over the measurement time. Changes in the azimuthal pointing dir-

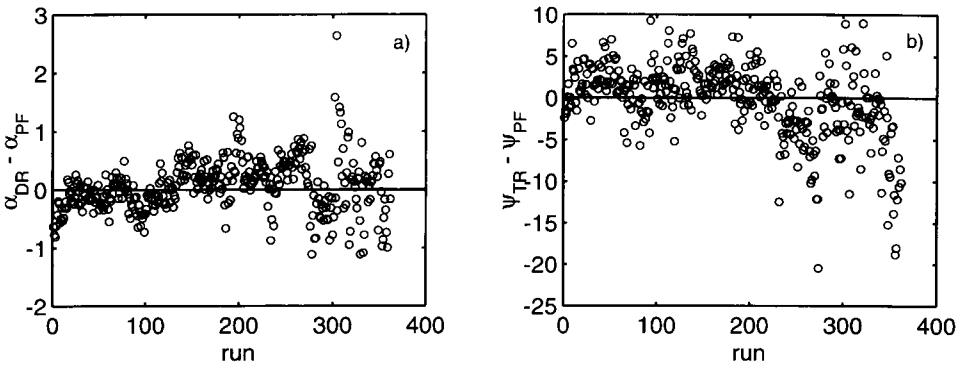

Figure 5. (a) The longitudinal (x-z plane) tilt angle due to sampling error with the DR method, computed as the difference between the DR method's longitudinal tilt angle and the tilt angle in the direction of the mean wind for each 15 min data run from the PF method, for each 15 min run. (b) The lateral tilt angle due to sampling error with the TR method, computed as the difference between the TR method's lateral tilt angle and the tilt angle perpendicular to the mean wind for each 15 min data run from the PF method.

ection of the anemometer, due for example to ship heading changes on a ship-based system, make no difference, as the surface has no unique direction. The tilts in this case will be measured relative to the ship. Measurements of the tilt angles using the PF method for a ship-based sonic anemometer may be problematic, however, due to large, azimuthally dependent vertical velocities caused by the ship's distortion of the flow field, and by slow continuous changes in the tilt of the ship over time.

The three methods described above are applicable for the rotation of velocity covariances into the streamline coordinate system. Moments that include buoyancy fluctuations strictly should be computed in a true vertical coordinate system. As discussed in Section 3, the dependence of the buoyancy flux on the tilt angle is small, except for near neutral conditions. For the greatest accuracy in the measurement of turbulent fluxes over sloping terrain, anemometers should be mounted as close to true vertical as possible for the determination of the buoyancy flux, and then later rotated into a streamline coordinate system to calculate the momentum flux.

Finally, we note that the PF technique can be used to test for flow distortion in the anemometer data. If the local terrain follows a plane surface so that the curvature is small, then the mean vertical velocity, normalized by the horizontal wind speed, should be a simple sinusoidal function of wind azimuth. Systematic deviations from this sinusoid (or systematic deviations from zero after the anemometer data have been corrected by the PF technique) would indicate mean vertical velocities resulting from flow distortion due to nearby structures.

Appendix A

Implementation of the PF method is simple if one has access to a linear algebra mathematics package (e.g., Matlab, Maple, Mathematica). Here we provide the code for determining the sonic tilt angles using Matlab.

The file vel.dat is an array of run-averaged velocity data, where the averaging is typically 15 to 60 min. The number of rows of data in vel.dat corresponds to the number of data runs. Each row of vel.dat consists of a set of three measured velocity components, u, v, and w, in the first, second, and third columns, respectively. The output file contains the tilt coefficients b_0, b_1, and b_2.

```
disp('Program to calculate sonic tilt angles')
fin = fopen('c:\matlab\vel.dat');                    %open input file
fout = fopen('c:\matlab\tilts.dat','w');             %open output file
z=fscanf(fid,'%g %g %g',[3,inf]);                    %read in velocity array
end;
u=z(1,:);
v=z(2,:);
w=z(3,:);
flen=length(u);
su=sum(u);                                           %sums of velocities
sv=sum(v);
sw=sum(w);
suv=sum(u*v');                                       %sums of velocity products
suw=sum(u*w');
svw=sum(v*w');
su2=sum(u*u');
sv2=sum(v*v');
H=[flen su sv; su su2 suv; sv suv sv2]               %create 3 × 3 matrix
g=[sw suw svw]'                                      %transpose of g
x=H\g                                                %matrix left division
fprintf(flist,'%10.5f %10.5f %10.5f %6.1f\n',x,fc);  %print b coeffs and # data
```

Acknowledgements

The authors wish to thank Drs. Christopher Fairall, Jeffrey Hare, Thomas Horst and William Massman for their constructive reviews of this manuscript, and to Dr. Andrew S. Kowalski for enlightening discussions. Funding for this research was provided by NOAA and by the Office of Naval Research through grant N00014-96-F-0010. The National Center for Atmospheric Research is sponsored by the U.S. National Science Foundation.

References

Chu, C. R., Parlange, M. B., Katul, G. G., and Albertson, J. D.: 1996, 'Probability Density Functions of Turbulent Velocity and Temperature in the Atmospheric Surface Layer', *Water Resour. Res.* **32**, 1681–1688.

Deacon, E. L.: 1968, 'The Leveling Error in Reynolds Stress Measurement', *Bull. Amer. Meteorol. Soc.* **49**, 836.

Dyer, A. J.: 1981, 'Flow Distortion by Supporting Structures', *Boundary-Layer Meteorol.* **20**, 243–251.

Dyer, A. J. and Hicks, B. B.: 1972, 'The Spatial Variability of Eddy Fluxes in the Constant Flux Layer', *Quart. J. Roy. Meteorol. Soc.* **98**, 206–212.

Finnigan, J. J.: 1983, 'A Streamline Coordinate System for Distorted Turbulent Shear Flows', *J. Fluid Mech.* **130**, 241–258.

Garratt, J. R.: 1992, *The Atmospheric Boundary Layer*, Cambridge University Press, 316 pp.

Geernaert, G. L.: 1988, 'Measurements of the Angle between the Wind Vector and the Wind Stress Vector in the Surface Layer over the North Sea', *J. Geophys. Res.* **93**, 8215–8220.

Goldstein, H.: 1981, *Classical Mechanics*, second edition, Addison-Wesley Publishing Company, 672 pp.

Grachev, A. A. and Fairall, C. W.: 2001, 'Upward Momentum Transfer in the Marine Boundary Layer', *J. Phys. Oceanog.*, accepted.

Hogstrom, U.: 1988, 'Non-Dimensional Wind and Temperature Profiles in the Atmospheric Surface Layer: A Re-Evaluation', *Boundary-Layer Meteorol.* **42**, 55–78.

Hogstrom, U.: 1990, 'Analysis of Turbulence Structure in the Surface Layer with a Modified Similarity Formulation for Near Neutral Conditions', *J. Atmos. Sci.* **47**, 1949–1972.

Hyson, P., Garratt, J. R., and Francey, R. J.: 1977, 'Algebraic and Electronic Corrections of Measured uw Covariance in the Lower Atmosphere', *J. Appl. Meteorol.* **16**, 43–47.

Kaimal, J. C. and Finnigan, J. J.: 1994, *Atmospheric Boundary Layer Flows*, Oxford University Press, 289 pp.

Kaimal, J. C. and Haugen, D. A.: 1969, 'Some Errors in the Measurement of Reynolds Stress', *J. App. Meteorol.* **8**, 460–462.

Kaimal, J. C., Wyngaard, J. C., Izumi ,Y., and Cote, O. R.: 1972, 'Spectral Characteristics of Surface Layer Turbulence', *Quart. J. Roy. Meteorol. Soc.* **98**, 563–589.

Lenschow, D. H., Wyngaard, J. C., and Pennell, W. T.: 1980: 'Mean-Field and Second-Moment Budgets in a Baroclinic Convective Boundary Layer', *J. Atmos. Sci.* **37**, 1313–1326.

McMillen, R. T.: 1988, 'An Eddy Correlation Technique with Extended Applicability to Non-Simple Terrain', *Boundary-Layer Meteorol.* **43**, 231–245.

Oost, W. A., Fairall, C. W., Edson, J. B., Smith, S. D., Anderson, R. J, Wills, J. A. B., Katsaros, K. B., and DeCosmo, J.: 1994, 'Flow Distortion Calculations and their Application in HEXMAX', *J. Atmos. Oceanic Tech.* **11**, 366–386.

Panofsky, H. A. and Dutton, J. A.: 1984, *Atmospheric Turbulence: Models and Methods for Engineering Applications*, John Wiley and Sons, New York, 397 pp.

Panofsky, H. A., Tennekes, J., Lenschow, D. H., and Wyngaard, J. C.: 1977: 'The Characteristics of Turbulent Velocity Components in the Surface Layer under Convective Conditions', *Boundary-Layer Meteorol.* **11**, 355–361.

Pielke, R. A.: 1984, *Mesoscale Meteorological Modeling*, Academic Press, Orlando, FL, 612 pp.

Pond, S.: 1968, Some Effects of Buoy Motion on Measurements of Wind Speed and Stress', *J. Geophys. Res.* **73**, 507–512.

Tanner, C. B. and Thurtell, G. W.: 1969, *Anemoclinometer Measurements of Reynolds Stress and Heat Transport in the Atmospheric Surface Layer*, University of Wisconsin Tech. Rep., ECOM-66-G22-F, 82 pp. [Available from US Army Electronic Command, Atmospheric Sciences Laboratory, Ft. Huachuca, AZ 85613.]

Wilczak, J. M., Edson, J. B., Hojstrup, J., and Hara, T.: 1999, 'The Budget of Turbulent Kinetic Energy in the Marine Atmospheric Surface Layer'. Chapter in G. L. Geernaert (ed.), *Air-Sea Exchange – Physics, Chemistry, Dynamics and Statistics*, Kluwer Academic Publishers, Dordrecht.

Wyngaard, J. C.: 1973, 'On Surface Layer Turbulence', in D. A. Haugen (ed.), *Workshop on Micrometeorology*, American Meteorological Society, Boston, MA, pp. 101–149.

Wyngaard, J. C.: 1981, 'The Effects of Probe-Induced Flow Distortion on Atmospheric Turbulence Measurements', *J. Appl. Meteorol.* **20**, 784–794.

Wyngaard, J. C. and Cote, O. R.: 1971, 'The Budgets of Turbulent Kinetic Energy and Temperature Variance in the Atmospheric Surface Layer', *J. Atmos. Sci.* **28**, 190–201.

Wyngaard, J. C., Cote, O. R., and Izumi, Y.: 1971, 'Local Free Convection, Similarity, and the Budgets of Shear Stress and Heat Flux', *J. Atmos. Sci.* **28**, 1171–1182.